

ms 14064  
COPY 2  
ACW: 223485

Vet

# Critical and Paramagnetic Spin Dynamics in an Antiferromagnetically Coupled Heisenberg Magnet: Results for $\text{RbMnF}_3$

A Cuccoli S W Lovesey and V Tognetti



June 1994

**DRAL is part of the Engineering and Physical  
Sciences Research Council**

The Engineering and Physical Sciences Research Council  
does not accept any responsibility for loss or damage arising  
from the use of information contained in any of its reports or  
in any communication about its tests or investigations

**Critical and Paramagnetic Spin Dynamics  
in an Antiferromagnetically Coupled Heisenberg  
Magnet: Results for RbMnF<sub>3</sub>.**

A. Cuccoli<sup>(1)</sup>, S. W. Lovesey<sup>(2)</sup> and V. Tognetti<sup>(1)</sup>

- (1) Department of Physics, University of Florence,  
L.E. Fermi 2, I-50125 Italy.
- (2) DRAL Rutherford Appleton Laboratory,  
Oxfordshire OX11 0QX, England, U.K.

Results are provided for the spin-spin response function of a three dimensional, antiferromagnetically coupled Heisenberg magnet, covering a range of temperatures from the critical temperature to deep in the paramagnetic phase. The wave vectors considered span the Brillouin zone. Damping rates are given at the zone centre and the antiferromagnetic ordering wave vector,  $\mathbf{w}$ , together with copious numerical results for the full response function. The calculations are based on the nonlinear, integral-differential equations obtained from so-called coupled-mode theory. In a confrontation between experimental and theoretical findings for RbMnF<sub>3</sub> nearly all aspects have a positive outcome. The main exception is found at  $T_c$  for wave vectors close to  $\mathbf{w}$ . Here, the measured response comprises three distinct components, reasonably ascribed to diffusive and oscillatory collective processes. In the corresponding predictions, the diffusive component is conspicuously missing. A less pronounced discrepancy is found at the antiferromagnetic zone boundary where, once again, there is more structure in the observed spectrum than in the calculated one.

## 1. Introduction

Over the past few decades, studies of the time-dependent properties of spin systems have played a significant rôle in the development of the current sophisticated theory of dynamical processes in condensed matter. Up to the end of the 60's, theoretical methods for spin systems tended to focus on the use of frequency moments, following very early ideas from Van Vleck and De Gennes, among others (for a review of this work see, for example, Marshall and Lowde 1968). These methods are not reliable at the critical temperature, where an infinite number of degrees of freedom are responsible for non-trivial features in the dynamics. Seminal work on this aspect of spin dynamics was reported by Wegner (1969), Résibois and DeLeener (1969) and Kawasaki (1968). It is now recongized, largely through the work of Hubbard (1971), that these developments all lead to the same system of closed non-linear equations for the time-dependent and wave vector-dependent spin-spin response function. Today, the equations are often referred to as the coupled-mode theory of the dynamical properties of spin systems.

Appropriate variants of coupled-mode theory have been successfully used to investigate properties of other highly correlated systems. Notable examples are models of the glass transition, and localization in the Anderson model. It is interesting to note in studies of fluids a strong similarity between the coupled-mode theory for fluctuations close to equilibrium and the direct-interaction theory of turbulence when the need for separate equations for the response and propagator are relaxed, i.e. the theory is reduced to the description of small fluctuation close to thermal equilibrium.

Applied to critical spin dynamics, coupled-mode theory is in accord with two other powerful approaches. One, scaling-theory, is a set of postulates that lead to predictions in the critical region from a knowledge of various properties in the hydrodynamical region. The renormalization group method provides asymptotic properties of the spin correlation function and explicit results for some critical exponents. Even though this method does not provide closed equations for the spin response function, it is particularly valuable since it alone is a systematic, perturbative

approach to critical phenomena in spin systems, and other models which display a continuous phase transition. Results derived for spin systems using dynamic scaling arguments and the renormalization group method are gathered, together with copious references, by Privman et al. (1990).

Although the pioneers of the coupled-mode approach focused attention on the critical properties of spin systems, there is a body of evidence to the effect that it provides an unrivalled account of paramagnetic fluctuations of short and long wavelengths (Hubbard 1971, Cuccoli et al. 1989, Cuccoli et al. 1990, and Westhead et al. 1991). Perhaps the most recent example of the reliability of coupled-mode theory outside the critical region is in its application to a spin chain at infinite temperature (Lovesey and Balcar, 1994). In this case, the theory provides insight to non-hydrodynamic behaviour observed in data from extensive computer simulations (Srivastava et al., 1994).

In this paper we continue the investigation of coupled-mode theory applied to spin systems by providing the first comprehensive study of an antiferromagnetically coupled Heisenberg magnet. Previous work on this system has focused on the critical and hydrodynamic limits (Wegner 1969, Huber and Krueger 1970, Bagnuls and Joukoff-Piette 1975). Here, we survey the spin-spin response function at the critical temperature,  $T_c$ , for all wave vectors in the Brillouin zone. In particular, at  $T_c$  we predict the behaviour of the van Hove response function,  $S(\mathbf{k}, \omega)$ , for the three special wave vectors,  $\mathbf{k}$ , near the chemical zone centre, the antiferromagnetic zone boundary, at which in the condensed phase the linear spin wave dispersion achieves its maximum value, and the antiferromagnetic ordering wave vector,  $\mathbf{w}$ . Above  $T_c$ , we show, starting deep in the paramagnetic phase and approaching  $T_c$ , how developing antiferromagnetic correlations manifest themselves in the time-dependent spin fluctuations. A combination of numerical and analytic methods of analysis are employed; the latter is used to demonstrate that, for the antiferromagnetically coupled system, coupled-mode theory is consistent with results derived with dynamic scaling arguments and the renormalization group method.

Where possible, theoretical results are compared with experimental data for  $S(\mathbf{k},\omega)$  obtain on  $\text{RbMnF}_3$ , using inelastic neutron scattering, by Tucciarone et al. (1971a,b). By and large, agreement between experimental and theoretical results is strikingly good. However, at  $T_c$  and for  $\mathbf{k}$  in the vicinity of the antiferromagnetic ordering wave there is an obvious disagreement; the experimental data for  $S(\mathbf{k},\omega)$  shows a three-peaked structure, namely, a central ( $\omega = 0$ ) diffusive mode and two side peaks attributed to collective spin oscillations, albeit heavily damped oscillations, while theoretical results for the appropriate wave vectors show only two collective mode peaks. The latter feature is consistent with results reported by Wegner (1969), independently confirmed by Hubbard (private communication). Here, we provide a more extensive picture of the disagreement between experimental and theoretical data. Since, to the best of our knowledge, it is the only example of its kind there is a case for new experiments; progress over the past two decades with neutron sources, instrumentation, and data analysis methods most likely mean that data for  $S(\mathbf{k},\omega)$  obtained by Tucciarone et al. (1971a,b) can be improved on (exceptional quality data can be obtained at  $\mathbf{k}\sim\mathbf{w}$  because there is next to no nuclear Bragg scattering contaminating the magnetic signal).

The next two sections describe the Heisenberg spin model and the corresponding coupled-mode theory (a detailed derivation of the theory and some of its properties is provided by Lovesey 1986, and Cuccoli et al. 1989). Decay rates near  $T_c$ , for the critical and hydrodynamical regions, are derived in §4. The findings demonstrate that coupled-mode theory is consistent with dynamic scaling arguments, and provide useful insight to the numerical results given in the subsequent two sections.

## 2. Model

Spin operators  $\mathbf{S}_a$  are placed on a lattice with  $N$  sites labelled by the index  $a$ . The spins interact through a Heisenberg interaction of strength  $J$ , so the model Hamiltonian is,

$$\mathcal{H} = J \sum_{a,b} \mathbf{S}_a \cdot \mathbf{S}_b \quad , \quad (2.1)$$

where the sum is over all nearest-neighbour pairs on the lattice.

We will study the time development of spatial Fourier components  $S(\mathbf{k})$  defined through,

$$S_a = (1/N) \sum_{\mathbf{k}} \exp(-i\mathbf{k} \cdot \mathbf{R}_a) S(\mathbf{k}). \quad (2.2)$$

The isothermal susceptibility is,

$$\chi(\mathbf{k}) = \frac{1}{3} (S(\mathbf{k}), \cdot S(-\mathbf{k})). \quad (2.3)$$

Here,  $(\cdot)$  denotes a Kubo relaxation function; for classical variables  $(A,B) = \langle AB \rangle / T$  where the angular brackets denote a thermal average, and  $T$  is the temperature ( $k_B = \hbar = 1$ ). The dynamic properties of (2.1) are studied in terms of the normalized relaxation function,

$$F(\mathbf{k}, t) = \frac{1}{3} (S(\mathbf{k}, t), \cdot S(\mathbf{k})) / \chi(\mathbf{k}), \quad (2.4)$$

where  $S(\mathbf{k}, t)$  is the standard Heisenberg time-dependent operator. The spectrum of neutrons inelastically scattered by spin fluctuations is proportional to,

$$S(\mathbf{k}, \omega) = (1/2\pi) \int_{-\infty}^{\infty} dt \exp(-i\omega t) F(\mathbf{k}, t). \quad (2.5)$$

In the context of neutron scattering,  $\omega$  is the energy transferred from the primary beam to the spin fluctuations. The concomitant change in the wave vector of the neutrons is  $\mathbf{k} = \mathbf{w} + \mathbf{q}$ , where  $\mathbf{w}$  is an antiferromagnetic ordering wave vector.

### 3. Coupled-Mode Theory

In view of the fact that coupled-mode theory for spin systems has recently been reviewed, we will provide in this section no more material beyond that required to define notation.

Coupled-mode theory is a closed set of equations for  $F(\mathbf{k}, t)$ . The latter is determined by,

$$\partial_t F(\mathbf{k}, t) = - \int_0^t dt' F(\mathbf{k}, t-t') K(\mathbf{k}, t'), \quad (3.1)$$

and the so-called memory function,  $K(\mathbf{k}, t)$ , is approximated by,

$$K(\mathbf{k}, t) = (2T / \chi(\mathbf{k})) \sum_{\mathbf{p}} \{\gamma_{\mathbf{p}-\mathbf{k}} - \gamma_{\mathbf{p}}\} F(\mathbf{p}, t) F(\mathbf{p} - \mathbf{k}, t) / (\mu_0 + \gamma_{\mathbf{p}}). \quad (3.2)$$

Here,  $\gamma_{\mathbf{k}}$  is a geometric factor that depends on the point group symmetry of the lattice; for a simple cubic lattice with a cell length  $a_0$ ,

$$\gamma_{\mathbf{k}} = \frac{1}{3} (\cos(a_0 k_x) + \cos(a_0 k_y) + \cos(a_0 k_z)) = 1 - \rho^2 k^2 + \dots.$$

The quantity  $\mu_0$  varies with temperature. In fact, the temperature scale is determined by the spherical model of spin correlations, namely,

$$(2rJS(S+1)/3T) = (1/N) \sum_{\mathbf{p}} (\mu_0 - \gamma_{\mathbf{p}})^{-1} = I(\mu_0), \quad (3.3)$$

in which  $r$  is the number of nearest neighbours ( $r = 6$ , s.c.), and the integral on the right-hand side is the standard extended Watson integral.

For a simple cubic lattice, the critical temperature,  $T_c$ , satisfies,

$$(4JS(S+1)/T_c) = 1.5164. \quad (3.4)$$

The spherical model susceptibility is,

$$\chi(\mathbf{k}) = \{N/2rJ(\mu_o + \gamma_{\mathbf{k}})\}. \quad (3.5)$$

In the key equations (3.1), (3.2) and (3.5) the wave vector variables  $\mathbf{p}$  and  $\mathbf{k}$  are general wave vectors in the Brillouin zone for the reciprocal lattice of the chemical structure.

As the critical temperature is approached from above  $\mu_o \rightarrow 1$ , and the susceptibility has a maximum at the antiferromagnetic ordering wave vector,  $\mathbf{w}$ , for which  $\gamma_{\mathbf{w}} = -1$ . Hence, for  $(\mu_o - 1) \ll 1$  we expand the geometric factor  $\gamma_{\mathbf{k}}$  in the susceptibility about  $\mathbf{w}$  using the small argument expansion, and find an Ornstein-Zernike form,

$$\chi(\mathbf{k}) = \{N/2rJ\rho^2(\kappa^2 + q^2)\}, \quad (3.6)$$

in which the inverse correlation length,  $\kappa$ , satisfies,

$$\rho^2 \kappa^2 = (\mu_o - 1), \quad (3.7)$$

and  $\mathbf{q}$  is measured relative to  $\mathbf{w}$ . For the spherical model, (3.7) leads to  $\kappa \sim (T - T_c)^\nu$  where the critical exponent  $\nu = 1$ .

#### 4. Decay Rates

For temperatures very close to  $T_c$ , such that  $\rho\kappa \ll 1$ , and very small wave vectors, the spin relaxation function  $F(\mathbf{k}, t)$  is expected to approach an exponential function of time for sufficiently long times. The associated decay rates can be estimated from equation (3.2) for the memory function.

To this end, in (3.2) shift the wave vector  $\mathbf{p}$  in the summation by an amount  $\mathbf{w}$ , and use the identity  $\gamma_{\mathbf{p}+\mathbf{w}} = -\gamma_{\mathbf{p}}$ . One finds,

$$K(\mathbf{k}, t) = (2T_c / \chi(\mathbf{k})) \sum_{\mathbf{p}} \{\gamma_{\mathbf{p}} - \gamma_{\mathbf{k}-\mathbf{p}}\} F(\mathbf{p} + \mathbf{w}, t) F(\mathbf{k} - \mathbf{w} - \mathbf{p}, t) / (\mu_o - \gamma_{\mathbf{p}}). \quad (4.1)$$

In the limit  $(\mu_o - 1) \ll 1$ , the denominator in the kernel emphasizes the region where  $p \ll 1$ , so it is appropriate to expand all functions in  $p$ . If the decay rates near  $k = 0$  and  $\mathbf{k} = \mathbf{w}$  are denoted by  $\Gamma_o$  and  $\Gamma$ , respectively, we obtain from (4.1) evaluated in the limit  $k \rightarrow 0$ ,

$$\Gamma_o(k) = (A/2) k^2 \int_0^q p^2 dp / \{\Gamma(p)(\kappa^2 + p^2)\}. \quad (4.2)$$

Here, the (non-universal) material constant,

$$A = (4T_c r J v_o / \pi^2), \quad (4.3)$$

where  $v_o$  is the volume of the chemical unit cell. It is prudent to express the decay rates in terms of a dimensionless parameter  $\theta = (k/\kappa)$ ; let,

$$\Gamma_o(k) = k^2 (A / \kappa)^{1/2} h_o(\theta),$$

and, near the ordering vector where  $\theta = (q/\kappa)$ ,

$$\Gamma(q) = \kappa^{3/2} (1 + \theta^2) A^{1/2} h(\theta). \quad (4.4)$$

From (4.2) we obtain the following integral equation for the dimensionless functions  $h(\theta)$  and  $h_o(\theta)$ ,

$$h_o(\theta) = \frac{1}{2} \int_0^{\infty} \zeta^2 d\zeta / \{(1 + \zeta^2)^2 h(\zeta)\}. \quad (4.5)$$

If we apply (4.1) to the case where  $\mathbf{k}$  is in the vicinity of  $\mathbf{w}$ , i.e.  $q \rightarrow 0$ ,

$$h(\theta) = \int_0^{\infty} \zeta^2 d\zeta / \{(1 + \zeta^2)[(1 + \zeta^2)h(\zeta) + \zeta^2 h_o(\zeta)]\}. \quad (4.6)$$

The pair of equations (4.5) and (4.6) determine the functions  $h_o(\theta)$  and  $h(\theta)$ .

In the critical limit,  $\theta \rightarrow \infty$ ,

$$\Gamma_o(q) = \Gamma(q) = q^{3/2} A^{1/2}. \quad (4.7)$$

From this result it follows that the dynamic critical exponent  $z = 3/2$ . In the opposite, hydrodynamical limit,  $\theta \rightarrow 0$ , and it can be shown that  $h_o(\theta)$  and  $h(\theta)$  tend to constant values determined by (4.5) and (4.6) evaluated with  $\theta = 0$ ;

$$\Gamma_o(k) = 0.553 k^2 (A / \kappa)^{1/2}, \quad (4.8)$$

and,

$$\Gamma(q) = 0.711 A^{1/2} \kappa^{3/2} (1 + (q / \kappa)^2).$$

Hence,  $\Gamma(\theta)$  decreases as the critical temperature is approached with a power law behaviour  $(T - T_c)^{2\nu}$ . On the other hand,  $\Gamma_o(k)$  increases with decreasing temperature with a power law  $(T - T_c)^{-\nu/2}$ . The decrease of  $\Gamma(\theta)$  as  $T$  approaches  $T_c$  is expected since  $\mathbf{w}$  is a Bragg position for the magnetic condensate.

## 5. Numerical Results

The numerical method for the solution of the coupled equations (3.1) and (3.2) is described by Cuccoli et al. (1989). Here, we provide results for the response function (2.5) for several different temperatures. All the results are for a nearest-neighbour exchange model, defined by (2.1), in which the spins are arranged on a simple cubic lattice with a cell length  $a_0$ .

At high temperatures, physical intuition leads one to expect that spin correlations will be strongest at quite short distances, probed by large wave vectors. This expectation is borne out by the results for  $T = 3.55T_c$  shown in fig. 1. In order to assess the influence of the correlations on  $S(\mathbf{k}, \omega)$  for  $\mathbf{k} = (\frac{1}{2}, \frac{1}{2}, \frac{1}{2})$  and  $\mathbf{k} = (1, 1, 1) = \mathbf{w}$ , measured in units of  $(\pi/a_0)$ , we have included in fig. 1 the function,

$$(2\pi\omega_0^2)^{-1/2} \exp(-\omega^2 / 2\omega_0^2), \quad (5.1)$$

in which  $\omega_0^2$  is the second frequency moment evaluated with the spherical model of static spin correlations, namely,

$$\omega_0^2(k) = \frac{8}{3} (r J \mu_0)^2 S(S+1)(1-\gamma_{\mathbf{k}})(1+\gamma_{\mathbf{k}}/\mu_0) \{1-1/\mu_0 I(\mu_0)\}, \quad (5.2)$$

and  $I(\mu_0)$  is defined in (3.3). The departures of  $S(\mathbf{k}, \omega)$  from the gaussian function are, indeed, most significant at the largest  $\mathbf{k}$ .

Antiferromagnetic correlations are not apparent in the results for  $T = 3.55T_c$  in as much that departures from a gaussian are more pronounced at  $\mathbf{w}$  than at the antiferromagnetic zone boundary  $(\frac{1}{2}, \frac{1}{2}, \frac{1}{2})$ . At the lower temperature  $T = 1.25 T_c$  this is no longer the case. Fig. 2 shows that at this temperature there is structure in  $S(\mathbf{k}, \omega)$  for  $\mathbf{k} = (\frac{1}{2}, \frac{1}{2}, \frac{1}{2})$  which is not present at  $\mathbf{k} = \mathbf{w}$ . To illustrate the antiferromagnetic character of the structure obtained at  $\mathbf{k} = (\frac{1}{2}, \frac{1}{2}, \frac{1}{2})$ , we have included the corresponding results for a ferromagnetically coupled system ( $J \rightarrow -J$  in equ. 2.1). For this case the ferromagnetic spin correlations probed at the ferromagnet zone boundary,  $\mathbf{k} = (1, 1, 1)$ , support a collective oscillation with a relatively long lifetime. The changes in energy scales for  $S(\mathbf{k}, \omega)$  seen in fig. 2 for different  $\mathbf{k}$ 's and different

exchange couplings can be understood from the behaviour of the second frequency moment (5.2); for a ferromagnetic exchange  $(1 + \gamma_{\mathbf{k}}/\mu_0) \rightarrow (1 - \gamma_{\mathbf{k}}/\mu_0)$ , while all other factors remain the same, and  $\mu_0 \sim 1$  near  $T_c$ . It is interesting to note that on setting  $\mu_0 = 1$  one finds  $\omega_0^2 \propto \epsilon_{\mathbf{k}}^2$ , where  $\epsilon_{\mathbf{k}}$  is the linear spin wave spectrum. For ferromagnetic (antiferromagnetic) coupling  $\epsilon_{\mathbf{k}}$  is a maximum at the zone boundary  $\mathbf{k} = \mathbf{w}$  ( $\mathbf{k} = (\frac{1}{2}, \frac{1}{2}, \frac{1}{2})$ ). Hence, the relatively narrow spectrum at  $\mathbf{k} = \mathbf{w}$  for an antiferromagnetic exchange coupling can be viewed as a signature of incipient antiferromagnetic ordering.

Lastly, we turn to results for  $T = T_c$ . Fig. 3 shows  $S(\mathbf{k}, \omega)$  with  $\mathbf{k}$  close to the zone centre and near  $\mathbf{w}$ . The antiferromagnetic correlations near  $\mathbf{w}$  produce a peak at a non-zero frequency, which gradually becomes less of a feature with increasing  $\mathbf{q} = \mathbf{k} - \mathbf{w}$ . The significant differences in  $S(\mathbf{k}, \omega)$  at  $\mathbf{k} \sim 0$  and  $\mathbf{k} \sim \mathbf{w}$  have been predicted by Wegner (1969). The widths of the spectra shown in Fig. 3 are consistent with a  $q^{3/2}$  scaling demonstrated in §4. Fig. 4 illustrates that at  $T_c$  there are no special features in the response function at the antiferromagnetic zone boundary, and the width of the spectrum is consistent with the estimate derived from (5.2).

## 6. Comparison with Experimental Data

Experimental studies of time-dependent spin fluctuations in magnetic systems which focus on critical phenomena are reviewed by Cowley (1987) and Collins (1989). Of the many materials included in these reviews, our attention is directed to the perovskite crystal  $\text{RbMnF}_3$ , which is an excellent example of a simple, isotropic antiferromagnetic salt. Indeed, the Hamiltonian for  $\text{RbMnF}_3$  is probably closer to that of an ideal model than is that of any other magnetic system (Collins, 1989).

Various properties of  $\text{RbMnF}_3$  are gathered in Table 1. The manganese ions are arranged on a simple cubic lattice, and the spin magnetic moments order antiferromagnetically below  $T_c$  with the moments directed along the sides of the magnetic unit cells. The experimental studies performed by Windsor and Stevenson (1966) show that the dominant exchange interactions are between nearest-neighbour ions, and there is next to no magnetic anisotropy. In consequence, the magnetic

properties of  $\text{RbMnF}_3$  are believed to be described by the Heisenberg Hamiltonian (2.1), to a very good approximation.

In the development of magnetic neutron scattering, an early detailed study of dynamic spin fluctuations in critical and paramagnetic regions was performed by Tucciarone et al. (1971 a,b) on  $\text{RbMnF}_3$ . We will review and contrast their findings at  $T_c$  and in the paramagnetic phase in the context of our findings for coupled-mode theory applied to the Heisenberg model (2.1). In our formulation of the coupled-mode theory one has set  $\eta = 0$ . Additionally, we have chosen to use the experimentally determined value of  $J$ , rather than opt for a value such that the spherical model  $T_c$  agrees with the observed value, cf. Table 1.

At  $T = T_c$ , the width of the response function near the antiferromagnetic Bragg peak is found experimentally to vary with the wave vector as  $q^z$  at small  $q$ , and  $z = 1.4 \pm 0.1$ . Above the critical temperature, antiferromagnetic Bragg reflections cease to exist as the lattice symmetry changes so as to make all sites equivalent. This means that there is no reason for the decay rate to go to zero as the wave vector  $q$ , measured relative to  $\mathbf{w}$ , goes to zero. The experiments show a dynamic response that is approximately of Lorentzian form at  $q = 0$ . The observed width varies with temperature according to a critical exponent of  $(1.46 \pm 0.13) \nu$ , whereas the coupled-mode theory, reported in §4, predicts an exponent of  $z\nu$  so that,  $z = 1.46 \pm 0.13$ , as shown in Table 2. This value is in satisfactory agreement with the prediction  $z = 3/2$ , and the experimental result obtained at  $T = T_c$ .

Turning to the results of our coupled-mode theory, fig. 5 shows the half-areas of  $S(\mathbf{k}, \omega)$  for three values of  $\mathbf{k}$  and five values of  $(T/T_c)$ . Theoretical and experimental results (Tucciarone et al. 1971 b) are in good agreement on an absolute basis. Note that the half-area at  $\mathbf{k} = \mathbf{w}$  decreases as  $T$  approaches  $T_c$ , while at the antiferromagnetic zone boundary  $\mathbf{k} = (\frac{1}{2}, \frac{1}{2}, \frac{1}{2})$  it increases with decreasing  $T$ . This behaviour is in accord with the predicted decay rates (for a Lorentzian response function the decay rate and half-area are the same). At  $T_c$ , we predict  $\Gamma(q) = q^{3/2} A^{1/2}$  for  $\rho q \ll 1$ , and the material parameters for  $\text{RbMnF}_3$  give the value  $A^{1/2} = 19.0 \text{ meV } \text{\AA}^{3/2}$ , whereas the observed half-area of the response function for  $\rho q \ll 1$  scales as  $q^{3/2}$ , as already noted,

and the constant of proportionality is  $16.0 \text{ meV } \text{\AA}^{3/2}$ . This tolerable agreement between experimental and theoretical quantities at  $T_c$  belies a significant difference in the observed and predicted frequency dependence of the response function.

At the critical temperature, the response function observed in the vicinity of  $\mathbf{w}$  is a three-peaked function of frequency. For moderate values of  $q$  the observed function exhibits a central ( $\omega = 0$ ) peak and two, equally displaced, side peaks ascribed to collective (spin wave) excitations. A finding of the data analysis is that a three-peaked structure persists at the smallest wave vectors,  $q \sim 0.05 \text{\AA}^{-1}$ , although it is obscured in the data by the resolution of the neutron spectrometer. Turning now to our predictions for the response function at  $T_c$ , fig. 3b shows that near  $\mathbf{w}$  there is no central peak, which one might associate with a spin diffusion process. A similar finding is reported by Wegner (1969). There is a similar, but less pronounced, discrepancy at the antiferromagnetic zone boundary. Looking at fig. 4, the corresponding data reported by Tucciarone et al. (1971b) shows a well defined peak at about 4 meV (we refer to their corrected and symmeterized data with the non magnetic background subtracted).

## 7. Conclusions and Discussion

Dynamic spin correlations in an antiferromagnetically coupled Heisenberg magnet have been studied from the critical temperature well into the paramagnetic phase. Attention is given to the spin-spin response function, or van Hove function,  $S(\mathbf{k}, \omega)$ . It is calculated for all vectors in the Brillouin zone. The outcome of the work is the first comprehensive study of critical and paramagnetic spin dynamics in an antiferromagnetically coupled Heisenberg magnet.

The calculations reported use the coupled-mode theory of spin dynamics. Applied to ferromagnetically coupled Heisenberg magnets, this theory is unmatched in its reliability, and range of application. Among its successes we mention correct predictions of decay rates (exponents and proportionality factors) at  $T_c$  and in the paramagnetic phase, and the influence of dipolar interactions (Frey et al. 1989, Lovesey 1993). In consequence, we have good reasons to be confident of the value of our reported findings for an antiferromagnetically coupled magnet.

By and large, there is very good agreement, on an absolute basis, between experimental and theoretical findings for  $\text{RbMnF}_3$ . Quantities which have been directly compared include the dynamic critical exponent,  $z$ , the temperature dependence of the decay rate at the antiferromagnetic ordering wave vector,  $\Gamma$ , and the half-areas at various wave vectors as a function of temperature in a range from just above  $T_c$  to deep in the paramagnet phase. However, the positive outcome of these comparisons to some extent paints a false impression. For, at  $T_c$  the observed and predicted spectral lines shapes in the vicinity of the antiferromagnetic ordering wave vector are distinctly different. The observed three-peaked structure is physically appealing, since it lends itself to an intuitive and sensible interpretation in terms of diffusive and collective oscillatory processes. The absence in the predicted line shape of a central, diffusive peak, perhaps, is a shortcoming of coupled-mode theory. If so, it is the only known significant shortcoming of coupled-mode theory applied to Heisenberg spin systems, and merits further experimental investigation. Bear in mind that  $\text{RbMnF}_3$ , by all accounts, is a near perfect example of a Heisenberg magnet. Even the ubiquitous dipolar interactions are irrelevant variables at  $T_c$ , according to a renormalization group analysis (Aharony, 1973).

### **Acknowledgements**

We benefited from a discussion about  $\text{RbMnF}_3$  with Dr. C. G. Windsor. Two of us (A.C. and V.T.) acknowledge, with thanks, the hospitality of DRAL during the course of carrying out the reported work.

**Table 1: Properties of RbMnF<sub>3</sub>**

Quantity	Symbol	Value
Chemical unit cell dimension	$a_0$	4.24Å
Critical temperature <sup>(1)</sup>	$T_c$	83K
Nearest neighbour exchange interaction	$J$	0.29 meV
Non-universal material constant in the damping rate	$A$	361.1 meV <sup>2</sup> Å <sup>3</sup>
Superlattice wave vector	$\mathbf{w}$	$(\pi/a_0)(1,1,1)$
Geometrical factor ( $\alpha = x,y,z$ )	$\gamma_{\mathbf{k}}$	$\frac{1}{3} \sum_{\alpha} \cos(a_0 k_{\alpha})$
Number of nearest neighbours	$r$	6
Spin magnitude	$S$	5/2

- (1) The quoted value of  $J$  and the spherical model relation (3.4) produce a critical temperature = 78K. Windsor and Stevenson (1966) report the value  $J = 0.29 \pm 0.03$  meV obtained from an analysis of the spin wave dispersion. All our results are provided as a function of the reduced temperature ( $T/T_c$ ), and  $A$  is calculated with  $T_c = 78$ K.

**Table 2**

Comparison of Critical Exponents of  $\text{RbMnF}_3$  as measured by Tucciarone et al. (1971a) with Predictions for the isotropic Heisenberg model (after Collins, 1989).

Exponent	Experiment	Calculation
$\gamma$	$1.366 \pm 0.024$	$1.388 \pm 0.003$
$\nu$	$0.701 \pm 0.011$	$0.707 \pm 0.003$
$\eta$	$0.055 \pm 0.010$	$0.037 \pm 0.009$
$z^{(1)}$	$1.46 \pm 0.13$	1.5

- (1) The value for the dynamic critical exponent,  $z = 3/2$ , is obtained from the coupled-mode equation, §4, and also dynamic scaling arguments and renormalization group calculations.

## Figure Captions

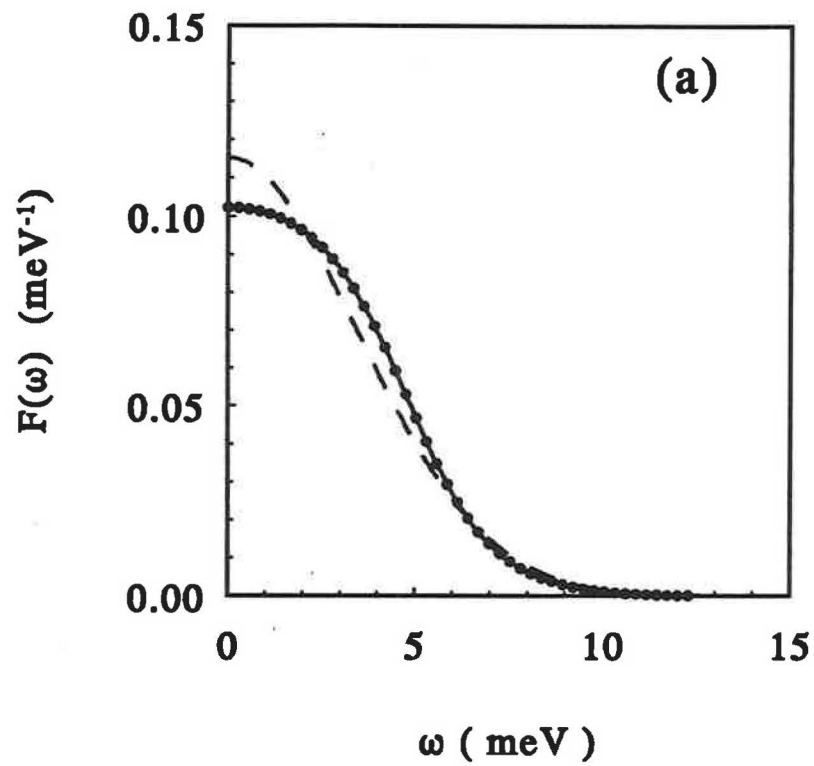
1.  $S(\mathbf{k},\omega)$  is displayed for two values of  $\mathbf{k}$  as a function of  $\omega$ . The wave vectors, measured in units of  $(\pi/a_0)$ , correspond to the antiferromagnetic zone boundary,  $\mathbf{k} = (\frac{1}{2},\frac{1}{2},\frac{1}{2})$ , and the antiferromagnetic ordering wave vector,  $\mathbf{k} = \mathbf{w} = (1,1,1)$ . The temperature  $T = 3.55T_c$ . Included in the figures is a gaussian function whose mean-square width is calculated from the second-frequency moment evaluated for the spherical model; see (5.1) and (5.2). The exchange parameter  $J = 0.29$  meV, and the spin  $S = 5/2$ .
2.  $S(\mathbf{k},\omega)$  is shown for  $T = 1.25T_c$  and ferro-(F) and antiferromagnetic (AF) coupling. Note that  $\mathbf{k} = \mathbf{w}$  is the ferromagnetic zone boundary. Parameters used, apart from the sign of  $J$ , are the same as in fig. 1.
3.  $S(\mathbf{k}, \omega)$  is displayed for  $T = T_c$ , and  $\mathbf{k}$  close to the Brillouin zone centre and the antiferromagnetic ordering wave vector  $\mathbf{w} = (1,1,1)$ . The wave vectors in units of  $(\pi/12a_0)$  are; (1) = (0,0,1), (2) = (0,1,1), (3) = (1,1,1), (4) = (11,12,12), (5) = (11,11,12) and (6) = (11,11,11). Other parameters are the same as those used in fig. 1.
4. The van Hove response function  $S(\mathbf{k},\omega)$  is shown for  $T = T_c$ , and  $\mathbf{k} = (\frac{1}{2},\frac{1}{2},\frac{1}{2})$  which is the antiferromagnetic zone boundary where the corresponding second-frequency moment, used to calculate the gaussian approximation to  $S(\mathbf{k},\omega)$ , achieves its maximum value in the Brillouin zone.
5. Widths at half-area of  $S(\mathbf{k},\omega)$ , examples of which are shown in figs. 1, 2 and 4, are given at three wave vectors and five reduced temperatures. The three wave vectors are  $\mathbf{k} = \mathbf{w}$ ,  $\mathbf{k} = (\frac{3}{4},\frac{3}{4},\frac{3}{4})$  and  $(\frac{1}{2},\frac{1}{2},\frac{1}{2})$ . Wave vectors are measured in units of  $(\pi/a_0)$  where  $a_0$  is the length of a side of the (cubic) chemical unit cell. When comparing these results with the corresponding experimental data for  $\text{RbMnF}_3$  reported by Tucciarone et al. (1971b) bear in mind that these authors quote wave vectors in units of  $(2\pi/a_0)$ .

## References

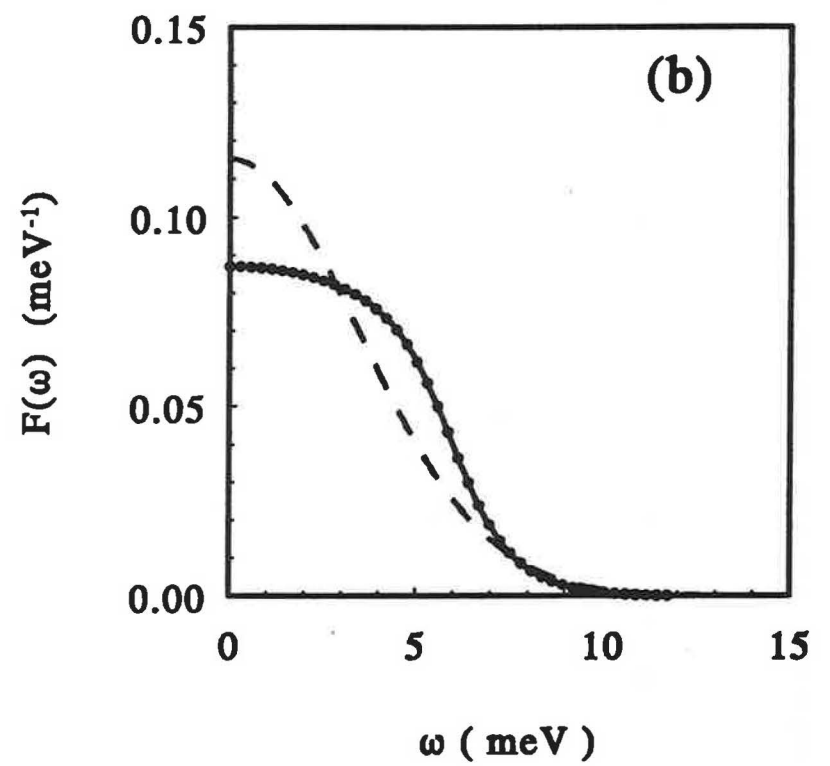
- Aharony, A., Phys. Rev. **B8** (1973) 3349
- Bagnuls, C., and Joukoff-Piette, C., Phys. Rev. **B11** (1975) 1986
- Collins, M.F., Magnetic Critical Scattering (O.U.P., N.Y., 1989)
- Cowley, R.A., in Methods of Experimental Physics, vol. 23 part C (Academic Press, Orlando, 1987)
- Cuccoli, A., Tognetti, V., and Lovesey, S.W., Phys. Rev. **B39** (1989) 2619
- Cuccoli, A., Tognetti, V., and Lovesey, S.W., J. Phys.: Condens. Matter **2** (1990) 3339
- Frey, E., Schwabl, F., and Thoma, S., Phys. Rev. **B40** (1989) 7199
- Hubbard, J., J. Phys. **C4** (1971) 53
- Huber, D.L., and Krueger, D.A., Phys. Rev. Lett. **24** (1970) 111
- Lovesey, S.W., and Balcar, E., J. Phys.: Condens. Matter **6** (1994) 1253
- Lovesey, S.W., J. Phys.: Condens. Matter **5** (1993) L251
- Lovesey, S.W., Condensed Matter Physics: Dynamic correlations, Frontiers in Physics, Vol. 61 (Benjamin/Cummings, 1986)
- Marshall, W., and Lowde, R.D., Repts. Prog. Phys. **B31** (1968) 705
- Privman, V., Hohenberg, P.C., and Aharony, A., Phase Transitions and Critical Phenomena, Vol. 14 edited by C. Domb and J. L. Lebowitz (Academic Press, London, 1990)
- Résibois, P., and De Leener, M., Phys. Rev. **178** (1969) 806; *ibid* **178** (1969) 819

- Srivastava, N., Liu, J-M., Viswanath, V.S., and Müller, G., *A. Appl. Phys.* to appear
- Tucciarone, A., Corliss, L.M., and Hastings, J.M., *J. Appl. Phys.* **42** (1971b) 1378
- Tucciarone, A., Lau, H.Y., Corliss, L.M., Delapalme., and Hastings, J.M., *Phys. Rev.* **B4** (1971a) 3206
- Westhead, D.R., Cuccoli, A., Lovesey, S.W., and Tognetti, V., *J. Phys.: Condens. Matter* **3** (1991) 5235
- Wegner, F., *Z. Phys.* **218** (1969) 260
- Windsor, C.G., and Stevenson, R.W.H., *Proc. Phys. Soc. (London)* **87** (1966) 501

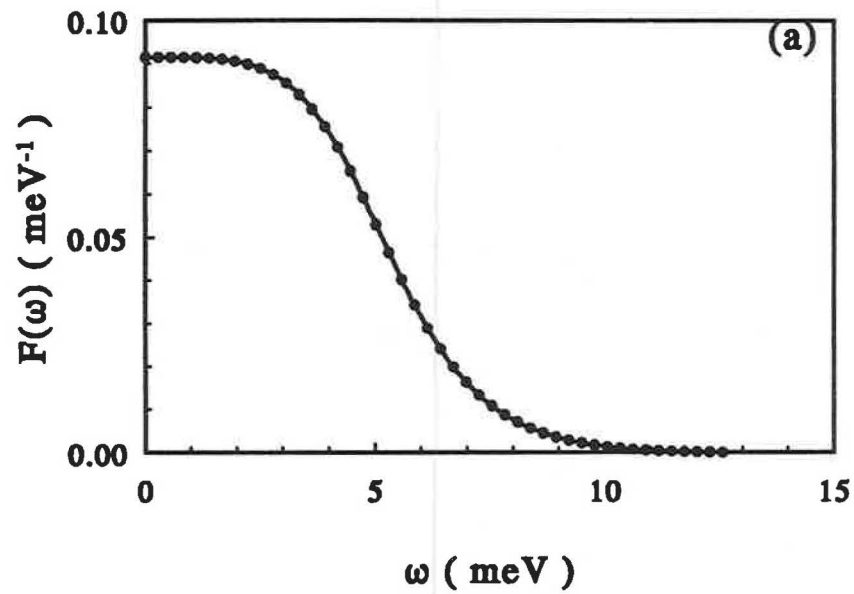
$T=3.55 T_c$   
 $\mathbf{k}=(0.5,0.5,0.5)\pi/a_0$



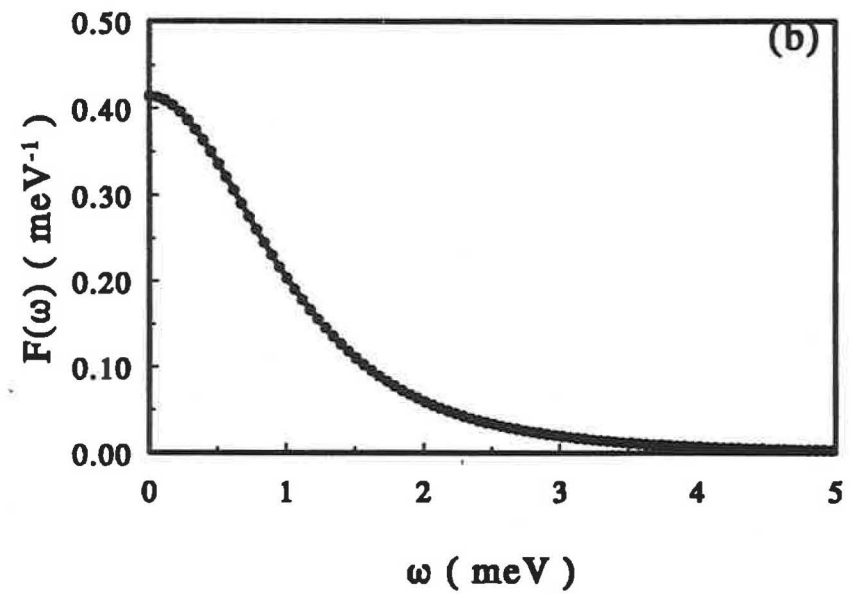
$T=3.55 T_c$   
 $\mathbf{k}=(1,1,1)\pi/a_0$



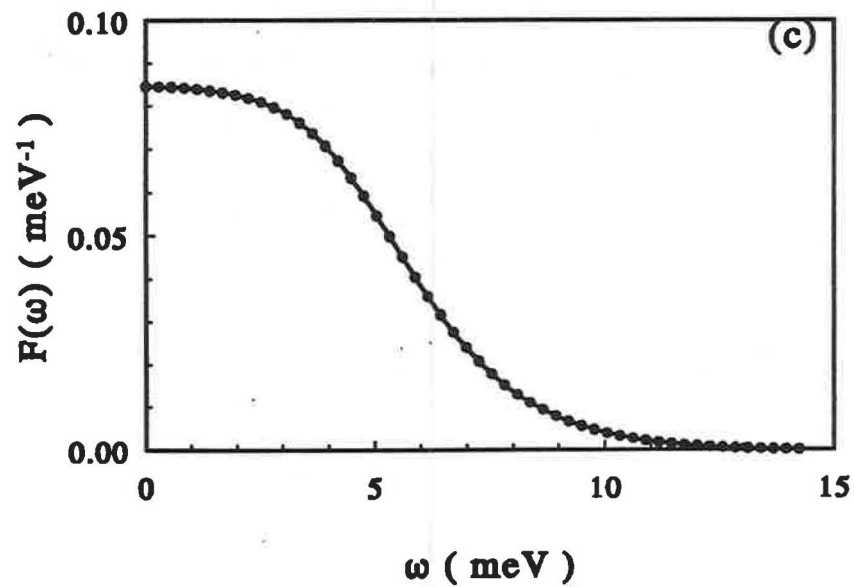
AF  $T=1.25 T_c$   
 $k=(0.5,0.5,0.5)\pi/a_0$



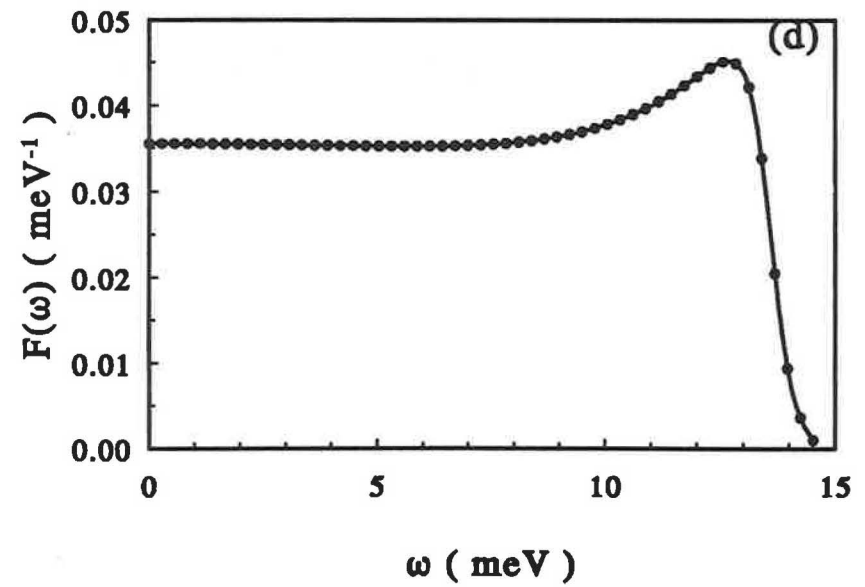
AF  $T=1.25 T_c$   
 $k=(1,1,1)\pi/a_0$



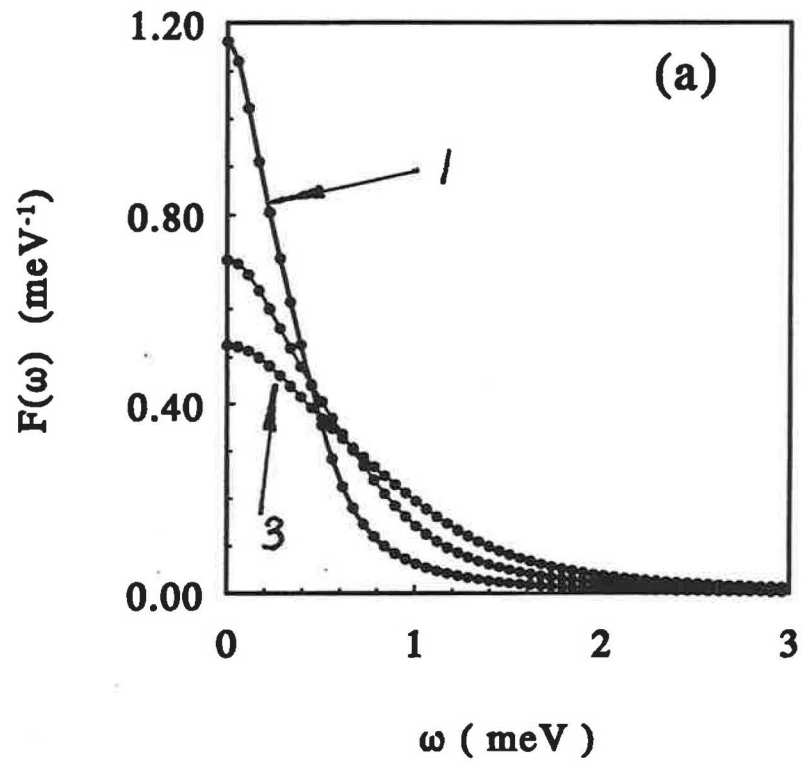
F  $T=1.25 T_c$   
 $k=(0.5,0.5,0.5)\pi/a_0$



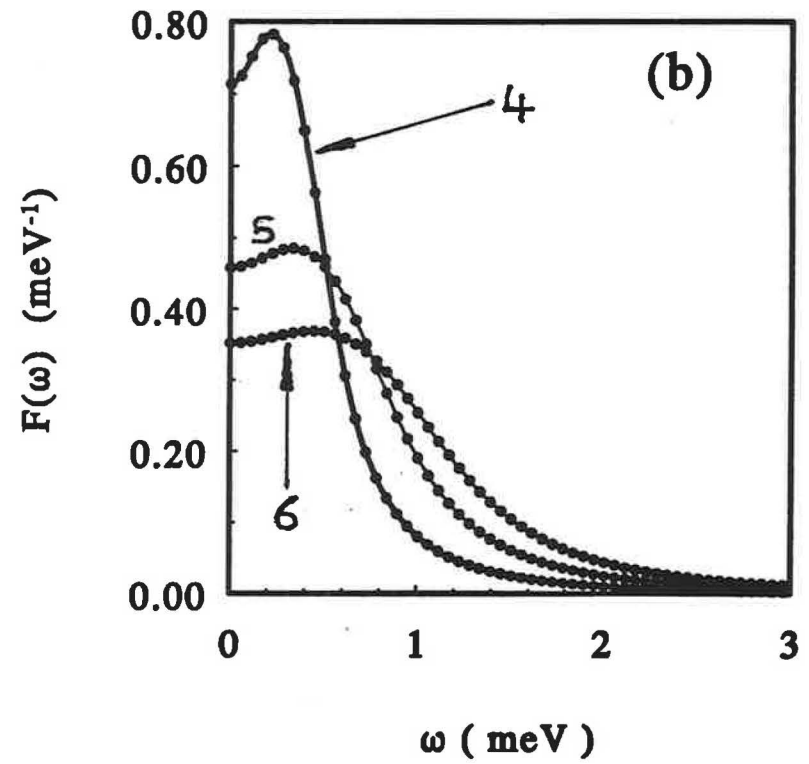
F  $T=1.25 T_c$   
 $k=(1,1,1)\pi/a_0$



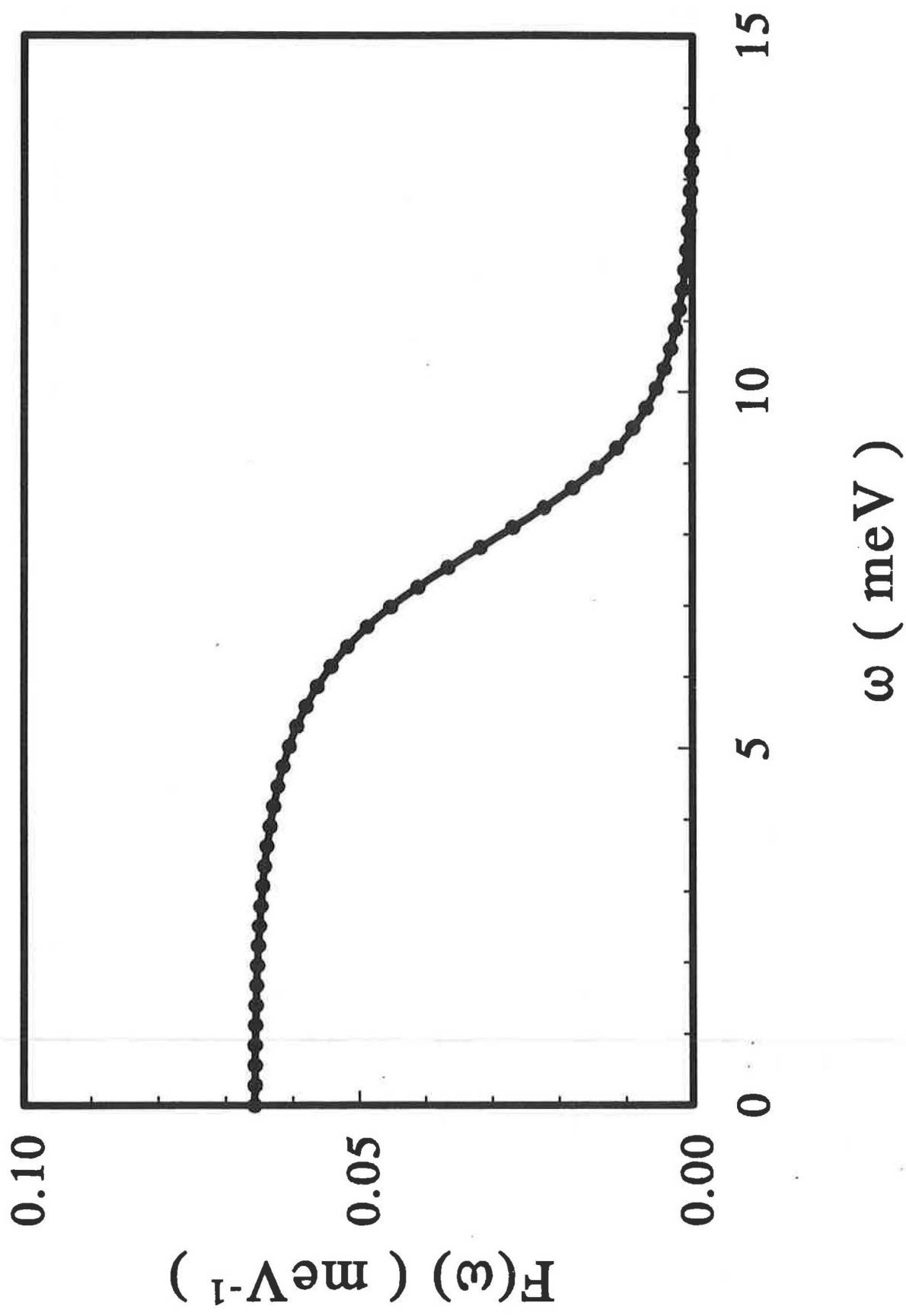
$T = T_c$



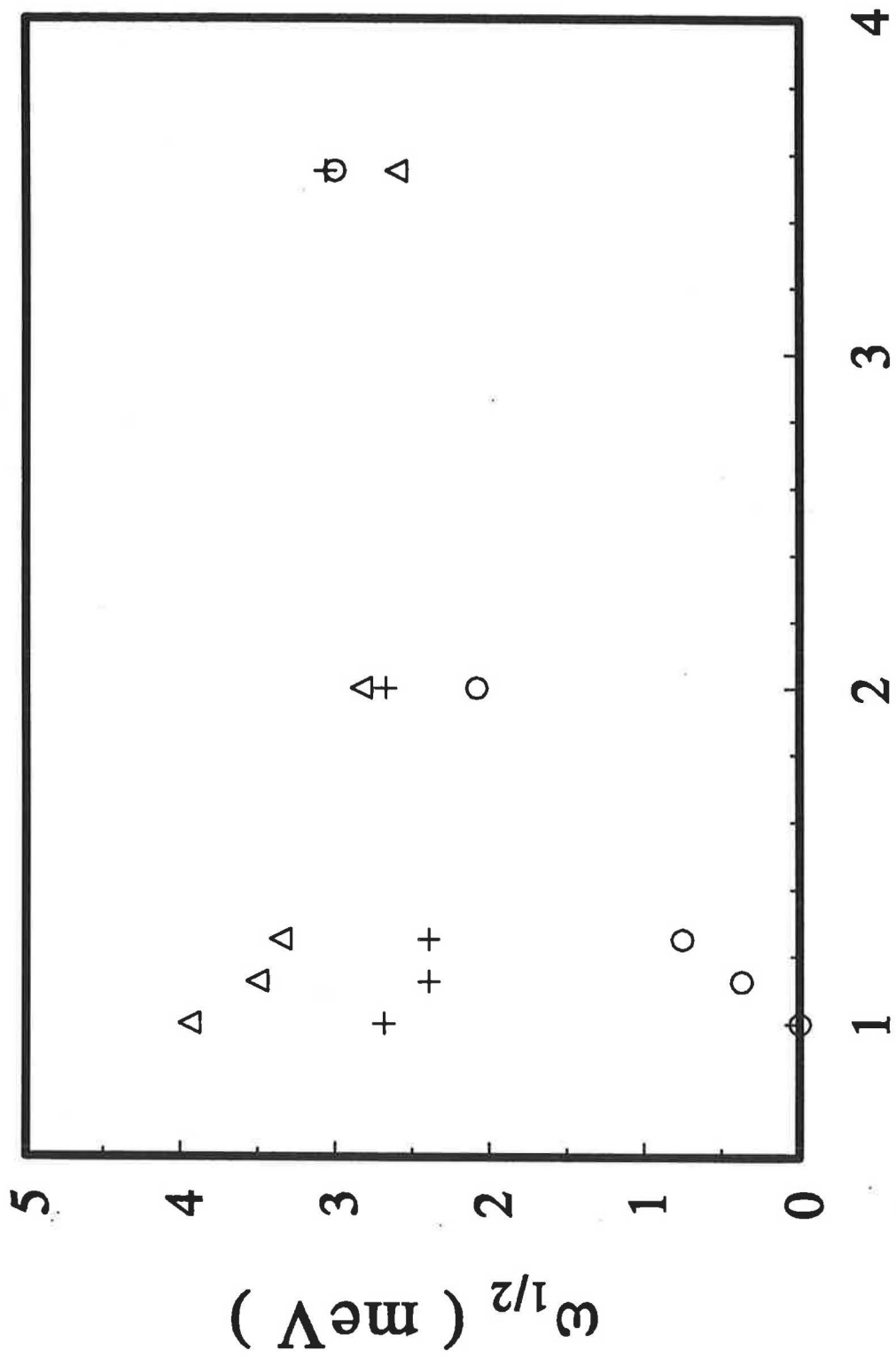
$T = T_c$



AF  $\Gamma = \Gamma_c$   
 $k = (0.5, 0.5, 0.5)\pi/a_0$



AF



T



